Infrared Spectra of Gallium Hydrides in Solid Hydrogen: $GaH_{1,2,3}$, $Ga_2H_{2,4,6}$, and the $GaH_{2,4}^-$ Anions

Xuefeng Wang and Lester Andrews*

Department of Chemistry, University of Virginia, McCormick Road, P.O. Box 400319, Charlottesville, Virginia 22904-4319

Received: May 20, 2003; In Final Form: September 30, 2003

Reactions of laser-ablated Ga atoms and normal hydrogen during co-deposition at 3.5 K give GaH as the major product and GaH_2, GaH_3, GaH_2^-, GaH_4^-, and Ga_2H_2 as minor products. Identifications are based on infrared spectra, isotopic substitution (D_2, $H_2 + D_2$ mixtures, HD), comparisons to earlier work, and frequencies calculated by density functional theory. Mercury arc radiation destroyed the GaH_2^- and GaH_4^- anions, decreased GaH and increased GaH_3, destroyed Ga_2H_2, and produced new bands due to Ga_2H_4, two Ga_2H_5 radical isomers, and Ga_2H_6. ArF laser irradiation at 193 nm was particularly effective in converting GaH to GaH_3 and to Ga_2H_6. The GaH_4^- anion absorptions in solid hydrogen are compatible with solid $NaGaH_4$ bands: Near-ultraviolet excitation of GaD_2^- with D_2 present increases GaD_4^- absorptions. Warming these samples to remove the H_2 matrix replaced sharp gallium hydride molecular absorptions with broad 1800−2000, 1300−1700, and 600−700 cm^{-1} bands due to higher oligomers containing terminal and bridged Ga−H bonds.

Introduction

Gallium and aluminum hydrides have much in common yet clear differences do exist.[1] The reactive transient monometal hydrides $MH_{1,2,3}$ are common to both metals:[2−6] The diatomic hydrides have been observed in the gas phase[7,8] and in solid matrixes,[2−6] but the dihydrides and trihydrides have been investigated only under matrix isolation conditions.[4−6] The tetrahydroaluminate anion, AlH_4^-, is well-known from the important reducing agent $LiAlH_4$, but the $NaGaH_4$ analogue is a much less common reagent.[9,10] Digallane is a stable gas-phase molecule, $H_2Ga(\mu\text{-}H)_2GaH_2$, but it decomposes to the elements above 243 K. However, digallane condenses into a molecular aggregate or oligomer with terminal Ga−H and bridging Ga−H−Ga bonds,[11,12] but dialane, $H_2Al(\mu\text{-}H)_2AlH_2$, is too reactive to survive in the gas phase and forms a three-dimensional network solid with bridging Al−H−Al bonds, $(AlH_3)_n$.[13−15] Group 3 hydrides are of interest as potential sources of the metal in chemical vapor deposition semiconductor device manufacture processes and for comparison of bonding and structure in the family series.

Very recently dialane was prepared in this laboratory through the reaction of laser-ablated Al atoms on condensation with pure H_2 at 3.5 K.[15] Ultraviolet photolysis converted the initial AlH formed to AlH_3 and diffusion in the soft hydrogen matrix fostered dimerization to Al_2H_6. Warming the sample to 7 K allowed the hydrogen matrix to evaporate and the AlH_3 and Al_2H_6 molecules to aggregate into a solid $(AlH_3)_n$ film with broad absorptions similar to those reported for the pure solid material.[16] Comparison of the seven fundamentals observed for Al_2H_6 in the terminal and bridged Al−H stretching and Al−H bending regions with frequencies calculated at several levels of electronic structure theory was important for this first identification of dialane.[15] The new Al_2H_4 molecule was also characterized in this work. Irradiation in the near-UV produced the same dialane products from thermal Al atoms in solid p-H_2.[17]

* To whom correspondence should be addressed. E-mail: lsa@virginia.edu.

Similar experiments with laser-ablated Ga and pure hydrogen were performed for proof of principle that Ga_2H_6 can be synthesized from the elements by this method and to prepare Ga_2H_4 and the isolated GaH_2^- and GaH_4^- molecular anions. Quantum chemical calculations show that dialane and digallane have the same dibridged structures as diborane.[17−20] Our Al/H_2 investigation found that AlH_2^- could not survive in solid hydrogen, but that AlD_2^- was trapped in solid deuterium and converted to AlD_4^- on 290-nm photolysis,[17] and we expect GaH_2^- to be less reactive.

Experimental and Theoretical Methods

The experiment for reaction of laser-ablated gallium atoms with hydrogen during condensation in excess argon, neon, and pure hydrogen has been described previously.[21−23] The Nd:YAG laser fundamental (1064 nm, 10 Hz repetition rate with 10 ns pulse width) was focused (10 cm f.l. lens) onto the gallium target (Johnson Matthey) in a rotating steel cup. Laser energy was varied from 10 to 30 mJ/pulse at the sample and maintained in this low range to keep the gallium target from melting. Laser-ablated metal atoms were co-deposited with 60 STPcc of pure normal hydrogen or deuterium (Matheson) or 120 STPcc of Ne/H_2 or Ne/D_2 onto a 3.5 K CsI cryogenic window for 25−30 or 50−60 min. Mixed isotopic HD (Cambridge Isotopic Laboratories) and $H_2 + D_2$ samples were used in different experiments. FTIR spectra were recorded at 0.5-cm^{-1} resolution on a Nicolet 750 with 0.1-cm^{-1} accuracy, using an MCTB detector. Matrix samples were annealed at different temperatures, using resistance heat, and selected samples were irradiated by filtered medium-pressure mercury arc (Philips, Sylvania, 175W) with the globe removed or 193-nm argon fluoride laser radiation (Optex, 30−80 mW) for 15-min periods.

Density functional theory (DFT) calculations of gallium hydride frequencies are given for comparison with experimental values. The Gaussian 98 program[24] was employed with the 6-311++G** basis set for hydrogen and gallium.[25] All geometrical parameters were fully optimized with the B3LYP and

10.1021/jp035393d CCC: $25.00
Published on Web 12/02/2003

TABLE 1: Infrared Absorptions (cm^{-1}) Observed from Reactions of Gallium Atoms and Dihydrogen Molecules in Excess Argon, Neon, and Pure Hydrogen

argon		neon			hydrogen		
H_2	D_2	H_2	HD	D_2	H_2	D_2	identification
					4087.3	2942.6	$(H_2)GaH_3$
					3972	2870	$(H^-)(H_2)_n$
					1995.0	1436.8	Ga_2H_6
					1980.5	1426.6	Ga_2H_5 (MB)[a]
					1975.7	1413.4	Ga_2H_6
					1967.0	1404.3	GaH_2H_5 (DB)[a]
					1943.9		Ga_2H_5 (MB)[a]
					1937.6		GaH_3 (site)
1922.7	1387.4	1933.4	1918		1928.7		GaH_3
			1396	1394.2		1391.1	GaD_3
					1883.5		Ga_2H_4 (site)
		1879.7			1875.3		Ga_2H_4
					1867.1		Ga_2H_4 (site)
		1867.5			1863.0		Ga_2H_4
				1356.6		1346.3	Ga_2D_4
						1338.4	Ga_2D_4
					1850.4		?
1803.7			1796.5		1822.0		GaH_2 (site)
1798.8		1822.0	1788.9		1814.9		GaH_2
	1307.8			1322.9,		1319.1	GaD_2 (site)
	1303.2			1318.9		1315.5	GaD_2
		1787.8			1783.0		$GaGaH_2$?
		1772.8			1773.8		GaH_4^-
					1765.7		GaH_4^-
				1285.6		1283.4	GaD_4^-
				1275.1		1272.6	GaD_4^-
1733.3			1294.0		1754.2		GaH_2 (site)
1727.2		1753.5	1290.1		1746.1		GaH_2
	1250.4			1268.1		1265.5	GaD_2 (site)
	1244.7			1264.2		1259.2	GaD_2
					1529.8		GaH (site)
1513.9		1530.7	1530.7		1516.9		GaH
						1104.2	GaD (site)
	1090.5		1099.9	1099.9		1091.5	GaD
					1463.5	1055.8	$(GaH)_n$
					1364.5		GaH_2
		1350.0	1357.9		1356.4		GaH_2^-
						981.2	GaD_2^-
			982.6	982.0		973.2	GaD_2^- site
					1272	922	Ga_2H_6
					1232		Ga_2H_5 (DB)[a]
					1202	859	Ga_2H_6
					1156.4	841.0	Ga_2H_5 (DB)[a]
1002.2		1034.6	984.8		1035.4		Ga_2H_2
					782.1		Ga_2H_5 (MB)[a]
	728.7			751.9		749.0	Ga_2D_2
					778.6		$GaGaH_2$
					774.5		$GaGaH_2$
						574.2	$GaGaH_2$
758		761			758.0		GaH_3
	545			542.9		542.7	GaD_3
					744.0		GaH_2
						529.6	GaD_2
					730.4		Ga_2H_4
717		721			719.2		GaH_3
	519			519.0		518.9	GaD_3
					671		Ga_2H_6
						482	Ga_2D_6

[a] Monobridged (MB) and dibridged (DB) isomers.

BPW91 density functionals,[26−30] and analytical vibrational frequencies were obtained at the optimized structures.

Results and Discussion

Matrix isolation infrared spectra of gallium hydrides will be assigned on the basis of isotopic substitution, theoretical calculations, sample irradiation, differences on annealing and changing ablation laser energy, and matrix host comparisons.

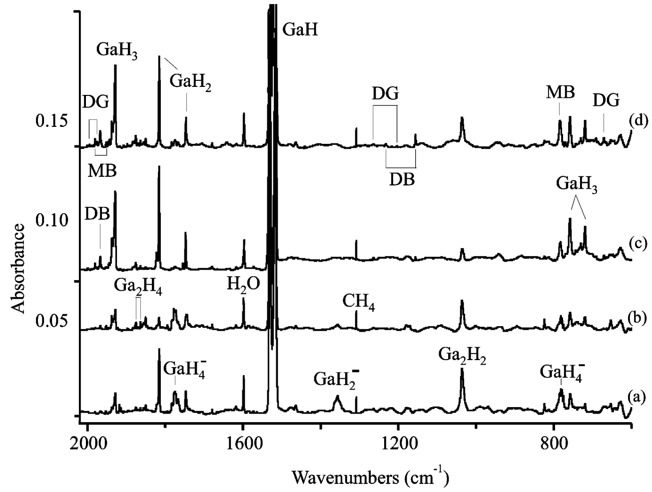

Figure 1. Infrared spectra in the 2020−600 cm^{-1} region for laser-ablated Ga atoms co-deposited with pure normal hydrogen at 3.5 K: (a) spectrum after sample deposition for 40 min, (b) after $\lambda > 470$ nm irradiation, (c) after $\lambda > 240$ nm irradiation, and (d) after annealing to 6.1 K.

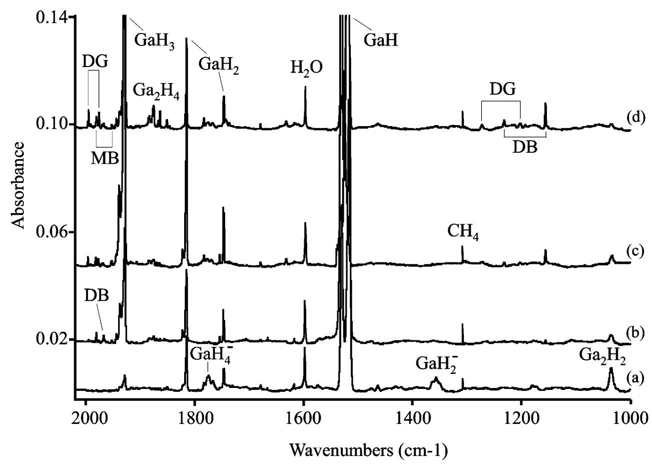

Figure 2. Infrared spectra in the 2020−1000 cm^{-1} region for laser-ablated Ga atoms co-deposited with pure normal hydrogen at 3.5 K: (a) spectrum after sample deposition for 30 min, (b) after $\lambda > 240$ nm irradiation, (c) after 193 nm irradiation, and (d) after annealing to 6.3 K.

Matrix samples from co-deposition of laser-ablated gallium atoms with pure H_2 at 3.5 K with subsequent annealing and visible-ultraviolet irradiation give a variety of reaction products. The infrared spectra are shown in Figures 1−8 for different experiments, and the product absorptions are listed in Table 1 for argon, neon, and hydrogen matrix experiments. These spectra reveal a trace (typically $A = 0.0005$) of Ga_2O (824.0 cm^{-1}) and a weak HGaOH absorption (1678.5 cm^{-1}) from reaction of gallium atoms with common system impurities.[21,31]

$GaH_{1,2,3}$. Gallium atoms were co-deposited with normal hydrogen at 3.5 K using five low ablation laser energies in order not to melt the metal target. A strong absorption at 1516.9 cm^{-1} with site at 1529.8 cm^{-1} appeared on deposition in pure hydrogen, doubled intensity on broadband photolysis, and decreased on annealing to 6.7 K. This band shifted to 1091.5 cm^{-1} (site at 1104.2 cm^{-1}) in pure D_2, giving a 1.390 H/D isotopic frequency ratio (Figures 1−3). Mixed $H_2 + D_2$ (35−65%) samples produce a strong band at 1514.0 cm^{-1} (Ga−H stretching region) and a weak band at 1091.7 cm^{-1} (Ga−D stretching region) with 6:1 relative intensity: Given the 2:1 relative infrared intensities of GaH and GaD (Tables 2, 3), this shows a 6:1 preference for the reaction of Ga with H_2 relative

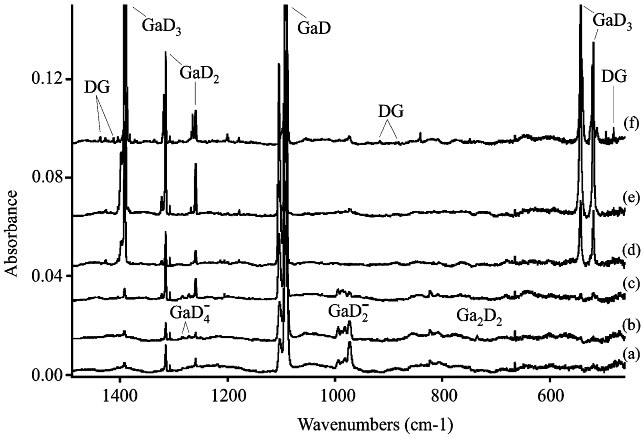

Figure 3. Infrared spectra in the 1490−460 cm^{-1} region for laser-ablated Ga atoms co-deposited with pure normal deuterium at 3.5 K: (a) spectrum after sample deposition for 40 min, (b) after annealing to 7.5 K, (c) after λ > 380 nm irradiation, (d) after λ > 240 nm irradiation, (e) after annealing to 8.7 K, and (f) after annealing to 9.4 K.

to D_2. The analogous bands with H_2 in neon at 1530.7 cm^{-1} and with D_2 in neon at 1099.9 cm^{-1} exhibit almost the same isotopic frequency ratio and photochemical behavior, and HD in neon reveals the same 1530.7- and 1099.9-cm^{-1} isotopic bands (Figures 4 and 5), indicating that the above bands are due to GaH and GaD. The absorptions of GaH and GaD in pure H_2, D_2, and $H_2 + D_2$ show slight matrix shifts. Experiments with H_2 (D_2) in argon produce weaker 1513.9 (1090.5)-cm^{-1} bands than two previous thermal metal investigations.[4,5] The absorptions for GaH and GaD are below the gas-phase fundamentals at 1547.0 and 1114.2 cm^{-1}, respectively.[7,8] The GaH absorption is dominant in pure H_2, and we observed no further reaction with H_2 on annealing. However λ > 240 nm photolysis induced GaH reactions with H_2 to give GaH_3 (Figure 1), but the conversion was more complete at λ = 193 nm (Figure 2). The neon-to-hydrogen-to-argon matrix shifts clearly show that the interaction of guest species with neon is less than that with H_2 and that with H_2 is less than that with argon.

A stronger band at 1814.9 cm^{-1} (site at 1822.0 cm^{-1}) tracks a weaker band at 1746.1 cm^{-1} (site at 1754.2 cm^{-1}) on deposition, decreases by 70% on λ > 530 nm photolysis, further decreases by 470-nm photolysis, but regenerates on 240-nm photolysis. The 1746.1-cm^{-1} band has a resolved splitting at 1747.6 cm^{-1}. The deuterium counterparts were found at 1315.5 (site at 1319.1 cm^{-1}) and 1259.2 cm^{-1} (site at 1265.5 cm^{-1}), giving isotopic frequency ratios of 1.380 and 1.387, respectively. With $H_2 + D_2$ the above bands with weak median bands at 1784.1 (Ga−H stretching region) and 1285.9 cm^{-1} (Ga−D region) with 3:1 relative intensity were obtained. The 1814.9- and 1746.1-cm^{-1} bands are assigned to symmetric and anti-symmetric Ga−H stretching modes for GaH_2. In solid neon, two bands at 1822.0 and 1753.5 cm^{-1} (GaH_2) shift to 1318.9 and 1264.2 cm^{-1} (GaD_2), and two strong median bands at 1788.9 and 1290.1 cm^{-1} with HD in neon are due to GaHD (Figure 3). The observation of very weak GaH_2 relative to GaHD indicates that the Ga + H_2 insertion reaction is the primary route to GaH_2. The absorptions for GaH_2 and GaD_2 trapped in argon in our experiments are basically the same as those observed by the Rice and Paris groups.[4,5]

A weak band at 1928.7 cm^{-1}, observed on deposition of Ga atoms with pure H_2, increased 5-fold on broadband photolysis and 2-fold further enhancement on 193-nm irradiation, but decreased on annealing to 6.7 K. Two strong bands at 758.0 and 719.2 cm^{-1} track with the upper band. These bands shift to 1391.1, 542.7, and 518.9 cm^{-1}, respectively, with pure D_2. In solid neon, similar bands with H_2 at 1933.4, 758.0, and 719.2 cm^{-1} and with D_2 at 1394.2, 542.9, and 518.9 cm^{-1} were observed. These bands are due to the absorptions of GaH_3 and GaD_3, which have been identified in solid argon.[6] Our argon matrix frequencies for GaH_3 are the same within $\pm$0.5 cm^{-1}.

A sharp weak 4087.3-cm^{-1} band appears on photolysis with the 1928.7-cm^{-1} GaH_3 band, and a 2942.6-cm^{-1} counterpart tracks with the 1391.1-cm^{-1} band in solid D_2 experiments. The 1.389 HD ratio is appropriate for an H−H stretching mode. Similar bands were observed at 4061.6 and 2919.6 cm^{-1} in alane experiments and assigned to the $(H_2)AlH_3$ and $(D_2)AlD_3$ complexes.[17] Note that the perturbation on the H−H fundamental near 4152 cm^{-1} is less in the $(H_2)GaH_3$ complex (65-cm^{-1} red shift) than in the $(H_2)AlH_3$ complex (90-cm^{-1} red shift).

DFT frequency calculations are in excellent agreement with experimental frequencies. At the B3LYP/6-311++G(d,p) level of theory the Ga−H stretching vibrations are predicted at 1560.4 cm^{-1} for GaH, 1845.9 and 1773.7 cm^{-1} (symmetric and antisymmetric modes) for GaH_2, and 1980.5 cm^{-1} (doubly degenerate (e′) mode) for GaH_3, which are overestimated by 1.9% (GaH), 1.1%, 1.3% (GaH_2), and 2.4% (GaH_3) compared with observations in neon. The computed bending modes for GaH_3 at 762.8 (e′) and 721.7 cm^{-1} (a_2'') are almost the same as neon bands at 761 and 721 cm^{-1}, respectively. As listed in Table 3, the BPW91 functional frequencies are slightly lower and closer to the experimental values. Supporting DFT and CCSD calculations for GaH_3 were also presented in the Paris report.[6]

Ga_2H_2. The cyclic molecule Ga(μ-H)$_2$Ga was trapped in the pure hydrogen matrix as a minor product. The 1035.4-cm^{-1} absorption shifted to 749.0 cm^{-1} with pure D_2 for the strong ring-stretching mode (Figures 1−3). These bands appeared on deposition, decreased on blue-UV photolysis, and restored partly on further annealing. It is interesting to note that the yield of Ga(μ-H)$_2$Ga is correlated to laser energy but not to GaH concentration: Higher ablation laser energy gives a higher yield of Ga(μ-H)$_2$Ga. The $H_2 + D_2$ experiments gave absorptions due to Ga(μ-H)$_2$Ga and Ga(μ-D)$_2$Ga and not Ga(μ-HD)Ga. Although strong GaH and GaD appeared on deposition and photolysis, dimerization is not the mechanism for formation of Ga(μ-H)$_2$Ga, which is produced from Ga_2 reaction with H_2.[32] The neon/H_2,D_2 experiments gave absorptions at 1034.6 (H) and 751.9 cm^{-1} (D), which are very close to pure H_2 and D_2 values and higher than argon matrix values at 1002.2 (H) and 728.7 cm^{-1} (D). The argon matrix bands appeared on annealing to 14−20 K. With HD in neon a band at 984.8 cm^{-1} was found for Ga(μ-HD)Ga, but absorptions due to Ga(μ-H)$_2$Ga and Ga(μ-D)$_2$Ga were not observed. This reaffirms the $Ga_2 + H_2$ reaction mechanism proposed by Himmel et al., who prepared Ga_2H_2 in very large yield.[32]

The Ga−H−Ga ring stretching mode observed in solid argon at 1002 cm^{-1} is about 33 cm^{-1} red-shifted from the neon matrix band. However, only 10−20 cm^{-1} red shifts were measured for the terminal Ga−H stretching vibrations of GaH, GaH_2, and GaH_3. It appears that the bridged Ga−H−Ga bond is more vulnerable to the polarizable matrix environment.

New absorptions at 1765.1, 1752.1 cm^{-1} and at 752.1, 747.0 cm^{-1} in solid argon have been recently assigned to the $GaGaH_2$ isomer based on their growth at the expense of Ga_2H_2 on λ = 546 nm photolysis and on comparison with B3PW91 calculated frequencies.[32] Our hydrogen matrix product bands at 1773.8, 1765.7 cm^{-1} and at 778.6, 774.5 cm^{-1} have a similar profile,

TABLE 2: Calculated Structures and Vibrational Frequencies (cm^{-1}) (B3LYP/6-311++G(d,p)) for Gallium Hydrides

species	state	Å, deg	rel energy[a]	freq, cm^{-1} (symmetry, intensities, km/mol)
GaH ($C_{\infty v}$)	$^1\Sigma$	GaH: 1.688		GaH: 1560.4 (874); GaD: 1111.8 (443)
GaH_2 (C_{2v})	$^2A_1$	GaH: 1.597 HGaH: 119.9	0.0	GaH_2: 1845.9 (b_2, 388), 1773.7 (a_1, 99), 733.7 (a_1, 126) GaD_2^-: 1319.7 (199), 1258.4 (51), 524.8 (64)
GaH_2^- (C_{2v})	$^1A_1$	GaH: 1.714 HGaH: 93.7	−29.1	GaH_2^-: 1405.6 (b_2, 1342), 1388.8 (a_1, 2163), 773.3 (a_1, 348) GaD_2^-: 1001.8 (666), 987.9 (860), 551.6 (163)
GaH_2^+ ($D_{\infty h}$)	$^1\Sigma_g^+$	GaH: 1.527 HGaH: 180.0	164.8	GaH_2^+: 2165.0 (σ_u, 0.3), 2059.8 (σ_g, 0), 671.6 (π_u, 31 × 2) GaD_2^+: 1553.1 (0), 1457.1 (0), 481.8 (19 × 2)
GaH_3 (D_{3h})	$^1A_1'$	GaH: 1.567 HGaH: 120.0		GaH_3: 1980.5 (e′, 263 × 2), 1976.7 (a_1', 0), 762.8 (e′, 154 × 2), 721.7 (a_2', 175) GaD_3: 1414.3 (139 × 2), 1398.3 (0), 545.6 (78 × 2), 521.1 (91)
GaH_4^- (T_d)	$^1A_1$	GaH: 1.623		GaH_4^-: 1761.8 (a_1, 0), 1684.2 (t_2, 368 × 3), 781.6 (e, 0 × 2), 729.9 (t_2, 410 × 3) $GaH_2D_2^-$: 1724.2 (341), 1681.9 (755), 1222.6 (197), 1203.7 (322), 756.9 (186), 683.9 (365), 677.1 (0), 584.4 (248), 538.1 (122) GaD_4^-: 1246.2 (0), 1200.1 (368 × 3), 552.9 (0 × 2), 526.5 (196 × 3)
Ga_2H_2 (D_{2h})	^1A_g	GaH: 1.879 HGaH: 108.4	0.0	Ga_2H_2: 1229.6 (a_g, 0), 1014.2 (b_{1u}, 1988), 879.8 (b_{3g}, 0), 857.8 (b_{2u}, 216), 202.0 (b_{3u}, 21), 187.6 (a_g, 0) Ga_2D_2: 870.1 (0), 722.6 (1009), 624.7 (0), 611.1 (110), 187.5 (0), 143.9 (11)
Ga_2H_2 (C_{2v})	$^1A_1$	GaH: 1.601 GaGa: 2.728 HGaH: 110.2	9.7	Ga_2H_2: 1834.9 (b_2, 394), 1822.2 (a_1, 553), 769.3 (a_1, 392), 350.6 (b_1, 82), 221.3 (b_2, 29), 174.5 (a_1, 13) Ga_2D_2: 1309.7 (202), 1294.5 (280), 549.3 (191), 254.4 (42), 173.4 (13), 159.2 (14)
Ga_2H_2 (C_{2h})	^1A_g	GaH: 1.630 GaGa: 2.630 HGaGa: 120.4	13.9	Ga_2H_2: 1694.0 (b_u, 1131), 1674.8 (a_g, 0), 489.8 (a_g, 0), 201.7 (a_u, 27), 159.1 (b_u, 43), 149.0 (a_g, 0) Ga_2D_2: 1206.9 (574), 1194.0 (0), 354.6 (0), 148.4 (0), 143.7 (14), 113.3 (22)
$H_2Ga(H)_2Ga$ (C_{2v})	$^1A_1$	GaH: 1.564 GaH′: 1.713 GaGa′: 2.811 HGaH: 125.4 H′GaH′:	0.0	Ga_2H_4: 1977.8 (b_1, 228), 1967.3 (a_1, 131), 1537.2 (a_1, 366), 1316.3 (b_2, 9), 1096.7 (a_1, 974), 1023.0 (b_2, 298), 761.9 (b_1, 108), 706.0 (a_1, 349), 698.2 (a_2, 0), 472.8 (b_2, 0), 201.8 (a_1, 0), 136.4 (b_1, 7)
$HGa(H)_3Ga$ (C_{3v})	$^1A_1$	GaH: 1.550 GaH′: 1.664 GaGa′: 2.555 HGaH′:	−0.5	Ga_2H_4: 2008.1 (a_1, 263), 1674.6 (a_1, 141), 1556.0 (e, 73 × 2), 827.8 (e, 18 × 2), 783.9 (a_1, 835), 761.6 (e, 193 × 2), 268.3 (e, 8 × 2), 240.7 (a_1, 30)
Ga_2H_4 (D_{2d})	$^1A_1$	GaH: 1.577 GaGa: 2.474 HGaH: 115.5	7.1	Ga_2H_4: 1932.8 (a_1, 0), 1929.6 (e, 82 × 2), 1913.9 (b_2, 439), 797.7 (a_1, 0), 718.6 (b_2, 522), 548.0 (e, 33 × 2), 295.7 (e, 44 × 2), 229.5 (a_1, 0), 187.2 (b_1, 0)
Ga_2H_5 (C_s)	$^2A'$	GaH: 1.557 GaH′: 1.759 Ga′H′: 1.778 Ga′H″: 1.585 Ga′H′Ga: 97.2 HGaH: 129.7 H′Ga′H″: 108.6	0.0	Ga_2H_5: 2021.2 (a′, 174), 1993.0 (a′, 108), 1847.1 (a′, 170), 1494.6 (a′, 21), 1235.4 (a′, 940), 1214.4 (a″, 215), 1203.4 (a″, 0), 731.0 (a′, 86), 697.1 (a′, 350), ..., 219.0.(a′, 0) Ga_2D_5: 1443.8 (97), 1414.2 (53), 1316.1 (89), 1058.5 (11), 878.5 (484), 866.2 (111), 851.8 (1), 521.8 (45), 498.7 (173), ..., 166.1 (2)
Ga_2H_5 (C_{2v})	$^2A_1$	GaH: 1.554 GaH′: 1.760 HGaH: 131.6 GaH′Ga: 95.5	1.0	Ga_2H_5: 2028.9 (b_1,377), 2022.9 (a_2,0), 2001.9 (a_1,3), 1992.4 (b_2,138), 1283.8 (536), 1234.5 (a_1,119), 744.5 (b_1,77), 708.0 (a_1,13), 645.8 (b_2,441), 580.4 (a_1,68), 470.9 (a_2,0), 341.9 (b_2,2), 287.4 (a_2,0), 224.2 (b_1,5), 187.5 (a_1,0)
Ga_2H_6 (D_{2h})	^1A_g	GaH: 1.552 GaH′: 1.758 HGaH: 130.4		Ga_2H_6: 2038.7 (b_{2u}, 371), 2031.5 (b_{1g}, 0), 2021.7 (a_g, 0), 2017.2 (b_{3u}, 130), 1517.9 (a_g, 0), 1331.9 (b_{3u}, 995), 1300.0 (b_{2g}, 0), 1249.4 (b_{1u}, 229), 784.3 (b_{2u}, 133), 768.3 (b_{3g}, 0), 734.5 (a_g, 0), 673.2 (b_{3u}, 551), 650.2 (b_{1u}, 120), 484.8 (b_{1g}, 0), 459.2 (a_u, 0), 398.4 (b_{2g}, 0), 230.4 (b_{2u}, 6), 229.7 (a_g, 0) Ga_2D_6: 1458.1 (196), 1452.3 (0), 1433.4 (0), 1429.6 (72), 1075.1 (0), 946.8 (518), 919.8 (0), 891.7 (122), 560.1 (67), 543.5 (0), 522.9 (0), 482.7 (279), 465.3 (60), 354.3 (0), 324.9 (0), 291.6 (0), 227.4 (0), 163.0 (3)

[a] Relative energy (kcal/mol).

but in contrast, these bands do not increase on 470-nm photolysis, which decreases Ga_2H_2 and virtually destroys GaH_2 in solid hydrogen. Furthermore, the yield of Ga_2H_2 in solid hydrogen is far less than that observed for the Ga_2 reaction in solid argon.[32] However, the weak, sharper 1783.0-cm^{-1} band increases relatively more on post photolysis annealing and this band may be due to the $GaGaH_2$ isomer.

We have no evidence for the HGaGaH isomer observed in solid argon[4,32] probably because Ga_2H_4 is favored in solid hydrogen. In fact the bands at 1875 and 1855 cm^{-1}, noted 4a by Himmel et al.[32] and characterized as having more hydrogen than Ga_2H_2, are assigned here to Ga_2H_4.

Ga_2H_4. Previous MP2 calculations for Ga_2H_4 found that the two bridge-bonded forms $H_2Ga(H)_2Ga$ and $HGa(H)_3Ga$ vie for the global minimum with the classical Ga_2H_4 (D_{2d}) structure 4 kcal/mol higher in energy and the D_{2h} form is slightly higher.[33,34] Our B3LYP calculations are in essential agreement (Table 2). We find evidence only for the strongest absorptions of Ga_2H_4: Weak bands observed on deposition at 1875.3, 1863.0, and 730.4 cm^{-1} decrease on UV photolysis, but reappear and increase on further annealing at the expense of GaH_2 absorptions (Figure 1). These bands are shown more clearly in the expanded scale spectra in Figure 6 where they increase when GaH_2 absorptions increase on $\lambda > 290$ nm irradiation and increase at the expense of GaH_2 absorptions on annealing to 5.4 K with infrared irradiation. The former bands shift to 1346.3 and 1338.4 cm^{-1} in pure D_2 (H/D ratios 1.393 and 1.392). These bands are in very good agreement with the strongest three absorptions predicted for Ga_2H_4 (D_{2d}) at 1929.6, 1913.9, and 718.6 cm^{-1} (Table 2). The e mode band at 1875.3 cm^{-1} is broader than the b_2 absorption at 1863.0 cm^{-1}. The two stretching modes are computed 45 and 51 cm^{-1} too high, comparable to the

TABLE 3: Calculated Structures and Vibrational Frequencies (BPW91/6-311++G(d,p)) for Gallium Hydrides

species	state	structure Å, deg	rel energy[a]	frequ, cm^{-1} (symmetry, intensities, km/mol)
GaH ($C_{\infty v}$)	$^1\Sigma$	GaH: 1.697		GaH: 1543.8 (820); GaD: 1099.9 (416)
GaH_2 (C_{2v})	$^2A_1$	GaH: 1.601	0.0	GaH_2: 1817.0 (b_2, 367), 1741.2 (a_1, 94), 712.4 (a_1, 113)
		HGaH: 120.0		GaD_2^-: 1299.0(188), 1235.3(49), 509.5(58)
GaH_2^- (C_{2v})	$^1A_1$	GaH: 1.719	−26.7	GaH_2^-: 1398.9 (b_2, 1237), 1373.0 (a_1, 2151), 745.2 (a_1, 340)
		HGaH: 93.3		GaD_2^-: 997.0 (613), 976.8 (1087), 531.6 (160)
GaH_2^+ ($D_{\infty h}$)	$^1\Sigma_g$	GaH: 1.534	163.0	GaH_2^+: 2131.7 (σ_u, 0.3), 2021.1 (σ_g, 0), 664.0 (π_u, 24 × 2)
		HGaH: 180.0		GaD_2^+: 1529.1 (0), 1429.7 (0), 476.3 (15 × 2)
GaH_3 (D_{3h})	$^1A_1'$	GaH: 1.572		GaH_3: 1953.0 (e′, 251 × 2), 1940.8(a_1', 0), 741.6 (e′, 139 × 2), 706.3 (a_2'', 154)
		HGaH: 120.0		GaD_3: 1394.7 (133 × 2), 1372.9 (0), 530.4 (70 × 2), 510.0 (80)
GaH_4^- (T_d)	$^1A_1$	GaH: 1.656		GaH_4^-: 1730.8 (a_1, 0), 1668.3 (t_2, 683 × 3), 763.2 (e, 0 × 2), 705.5 (t_2, 362 × 3)
				GaD_4^-: 1224.4 (0), 1188.8 (368 × 3), 539.8 (0 × 2), 508.9 (172 × 3)
Ga_2H_2 (D_{2h})	^1A_g	GaH: 1.878		Ga_2H_2: 1229.9 (a_g, 0), 1014.9 (b_{1u}, 1987), 881.0 (b_{3g}, 0), 852.1 (b_{2u}, 216), 199.4 (b_{3u}, 22), 187.7 (a_g, 0)
		HGaH: 108.4		Ga_2D_2: 870.3 (0), 723.0 (1009), 625.6 (0), 611.4 (110), 187.7 (0), 142.1 (11)
Ga_2H_4 (D_{2d})	$^1A_1$	GaH: 1.583		Ga_2H_4: 1902.9 (e, 258 × 2), 1901.0 (a_1, 0), 1884.2 (b_2, 403), 776.1 (a_1, 0), 695.3 (b_2, 447), 539.8 (e, 27 × 2), 289.6 (e, 37 × 2), 227.2 (a_1, 0), 212.7 (b_1, 0)
		GaGa: 2.464		
		HGaH: 115.4		
Ga_2H_6 (D_{2h})	^1A_g	GaH: 1.556		Ga_2H_6: 2009.4 (b_{2u}, 344), 2001.7 (b_{1g}, 0), 1986.8 (a_g, 0), 1983.2 (b_{3u}, 129), 1488.9 (a_g, 0), 1296.0 (b_{3u}, 852), 1290.1 (b_{2g}, 0), 1247.4 (b_{1u}, 188), 739.8 (b_{2u}, 106), 737.6 (b_{3g}, 0), 711.1 (a_g, 0), 651.1 (b_{3u}, 551), 630.4 (b_{1u}, 120), 472.5 (b_{1g}, 0), 447.8 (a_u, 0), 401.6 (b_{2g}, 0), 226.1 (b_{2u}, 6), 214.5 (a_g, 0)
		GaH′: 1.761		Ga_2D_2: 1437.2 (181), 1431.1 (0), 1408.7 (0), 1405.6 (72), 1054.7 (0), 921.4 (518), 913.0 (0), 890.1 (122), 528.3 (67), 521.8 (0), 506.0 (0), 466.9 (279), 451.3 (60), 345.5 (0), 316.8 (0), 294.0 (0), 224.0 (0), 151.7 (3)
		HGaH: 130.7		

[a] Relative energy (kcal/mol).

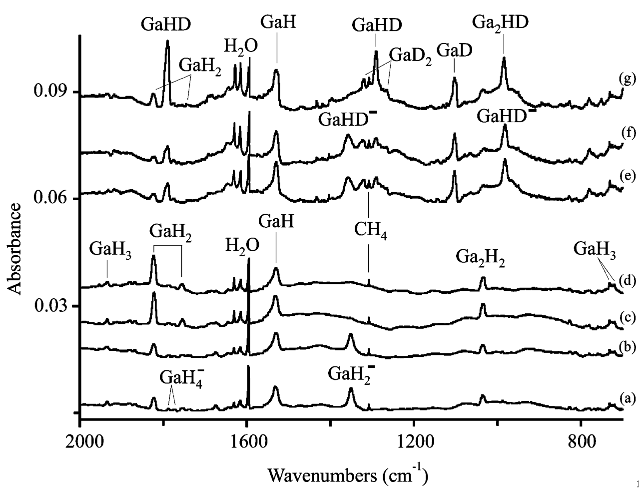

Figure 4. Infrared spectra in the 2000−700 cm^{-1} region for laser-ablated Ga atoms co-deposited with hydrogen in neon at 3.5 K: (a) spectrum after sample deposition of 5% H_2 in neon for 60 min, (b) after annealing to 7 K, (c) after 240−380 nm irradiation, and (d) after annealing to 8 K; (e) spectrum after sample deposition of 5% HD in neon for 60 min, (f) after annealing to 7 K, and (g) after 240−380 nm irradiation.

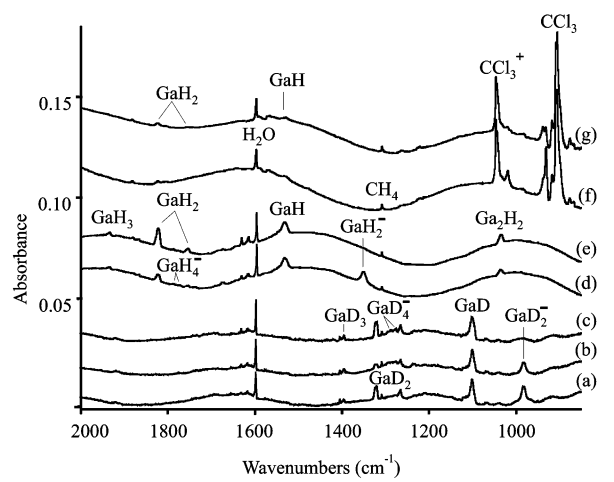

Figure 5. Infrared spectra in the 2000−860 cm^{-1} region for laser-ablated Ga atoms co-deposited with hydrogen in neon at 3.5 K: (a) spectrum after sample deposition of 5% D_2 in neon for 60 min, (b) after λ > 380 nm irradiation, and (c) after λ > 290 nm irradiation; (d) spectrum after sample deposition of 5% H_2 in neon for 60 min and (e) after 240−380 nm irradiation; (f) spectrum after deposition of 5% H_2 and 0.1% CCl_4 in neon and (g) after 240−380 nm irradiation.

predictions for GaH_3 (+53 cm^{-1}) and GaH_2 (+31, +27 cm^{-1}). We note that Ga_2H_4 absorptions appear 50−60 cm^{-1} above GaH_2, almost the same relationship found for Al_2H_4 and AlH_2.[15,17]

$H_2Ga(\mu\text{-}H)_2GaH_2$. The digallane molecule has been synthesized and identified in the gas phase at near-ambient temperatures and in low-temperature nitrogen and argon matrixes.[11,12] However, the isolated digallane molecule was not formed in solid argon by reaction of Ga or Ga_2 with H_2.[4,5,32] The solid hydrogen matrix provides the best chance to form digallane from the elements based on the fact that dialane was prepared with this method.[15,17] Two weak bands at 1995.0 and 1975.7 cm^{-1} in the Ga−H stretching region, two broad bands at 1272 and 1202 cm^{-1} in the bridged Ga−H−Ga ring stretching region, and a sharp band at 671 cm^{-1} in the GaH_2 bending region track together on sample irradiation and annealing, and can be assigned to $H_2Ga(\mu\text{-}H)_2GaH_2$ in solid hydrogen. First, this group of absorptions appeared together on broadband UV photolysis, increased further on 193-nm irradiation, increased together on 6.1−6.3 K annealing, and decreased on 6.7−6.8 K annealing as GaH_3 increased on photolysis and then decreased on annealing (Figures 1 and 2). The expanded scale spectra in Figure 6 show the two terminal GaH_2 stretching modes more clearly. The Ga_2H_6 bands first appear on full arc irradiation when GaH_3 bands are intense. One must conclude that dimerization of GaH_3 formed Ga_2H_6 in this process. Second, with pure D_2 the bands shift to 1436.8, 1413.4, 922, 859, and 482 cm^{-1}, respectively (Figure 3), and give the H/D ratios 1.389, 1.398, 1.380, 1.399, and 1.392. The H/D frequency ratios are comparable to these modes in GaH_3. Third, the absorptions of $H_2Ga(\mu\text{-}H)_2GaH_2$ in solid H_2 are in excellent agreement with gas-phase values.[12] The terminal Ga−H stretching vibrations

TABLE 4: Comparison of B_2H_6, Al_2H_6, and Ga_2H_6 Frequencies

	B_2H_6			Al_2H_6		Ga_2H_6		
mode	calcd[a]	gas[b]	H_2 matrix[c]	calcd[a]	H_2 matrix[d]	calcd[a]	gas[e]	H_2 matrix[f]
ν_8 (b_{1u})	2698(186)	2613	2604	1989(419)	1932	2039(371)	1993	1995
ν_{16} (b_{3u})	2594(149)	2518	2516	1966(126)	1915	2017(130)	1976	1976
ν_{13} (b_{2u})	1982(9)	1924		1292(352)	1268	1249(229)	1202	1202
ν_{17} (b_{3u})	1703(471)	1615	1596	1483(1096)	1408	1332(995)	1273	1232

[a] Calculated B3LYP/6-311++G**. [b] Reference 35. [c] Wang, X.; Andrews, L. To be submitted for publication. [d] Reference 15. [e] Reference 12. [f] This work.

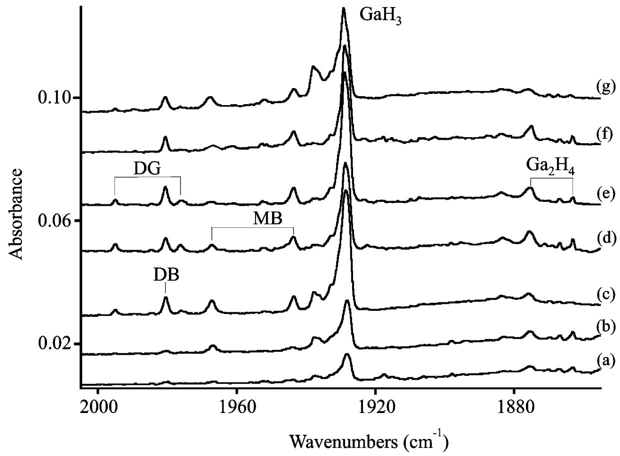

Figure 6. Infrared spectra in the 2005−1855 cm^{-1} region for laser-ablated Ga atoms co-deposited with pure normal hydrogen at 3.5 K: (a) spectrum after sample deposition for 30 min, (b) after λ > 240 nm irradiation, (c) after λ > 240 nm irradiation, (d) after IR irradiation with the sample at 5.4 K, (e) after annealing to 6.5 K, (f) after annealing to 7.5 K with a neon overcoat, and (g) after λ > 240 nm irradiation.

at 1995.0 and 1975.7 cm^{-1} and Ga−H−Ga bridge modes at 1272 and 1202 cm^{-1} are almost identical to gas-phase values at 1993, 1976, 1273, and 1202 cm^{-1}. Finally our DFT calculations support this assignment: The B3LYP functional gives two terminal Ga−H stretching modes at 2038.7 and 2017.2 cm^{-1}, overestimated by 2%, and two Ga−H−Ga ring stretching modes at 1332 and 1249 cm^{-1}, overestimated by 4% from the gas-phase values.

It is interesting to note that the relative intensity of the strong parallel bridged H stretching mode is less than predicted by DFT frequency calculations; however, the analogous B−H−B ring stretching mode observed for $H_2B(\mu\text{-}H)_2BH_2$ in solid hydrogen is similar to gas-phase observations.[35] The relative intensities of two modes in $H_2Al(\mu\text{-}H)_2AlH_2$ are close to theoretical calculations.[15] A matrix effect must be considered: The bond strength of Ga−H−Ga is weaker than Al−H−Al and much weaker than B−H−B and the former is accordingly more affected by the matrix.

Table 4 lists the terminal M−H stretching and M−H−M ring stretching vibrations observed for three bridged species, and compares calculated frequencies and relative intensities. The terminal M−H stretching modes for B_2H_6 at 2604 and 2516 cm^{-1} are much higher than those for Al_2H_6 at 1932 and 1915 cm^{-1} and for Ga_2H_6 at 1995 and 1976 cm^{-1} because the B−H bond is the strongest. Note that from Al−H stretching vibrations, the Ga−H stretching modes are up 60 cm^{-1}, which is because of bond-length contraction from Al−H to Ga−H. However, the parallel M−H−M ring-stretching frequencies (b_{3u} mode) continue to red-shift, indicating that the bridged M−H−M bonds get weaker from B to Al to Ga. Also the Ga−(H)$_2$−Ga subunit appears to interact more strongly with the matrix as this sustains a decrease in intensity.

Ga_2H_5 Radical. The presence of GaH_2 and GaH_3 in these samples suggests that Ga_2H_5 might also be formed in association reactions on annealing. Our B3LYP calculations find the dibridged Ga_2H_5 structure consisting of Ga_2H_6 without one terminal bond to be 1.0 kcal/mol lower in energy than the Ga_2H_5 structure with a 2.605 Å Ga−Ga bond replacing one bridging hydrogen (Table 2). Irradiation at λ > 290 nm increases GaH_2 and GaH_3 and gives new associated 1980.5-, 1943.9-, and 782.1-cm^{-1} absorptions and subsequent annealing produces new associated 1967.0-, 1232-, and 1156.4-cm^{-1} absorptions, which appear before the Ga_2H_6 bands (Figures 1, 2, and 6). The 1943.9-cm^{-1} band is due to a terminal GaH_2 subunit and could be either Ga_2H_5 isomer, but the sharp 1156.4-cm^{-1} band is due to a Ga−H−Ga bridge-stretching mode, with 1156.4/841.0 = 1.375 frequency ratio, and the second 1232-cm^{-1} band requires two bridging hydrogens. In addition, the dibridged isomer has the stronger computed bridge stretching mode. The 1967.0-, 1232-, and 1156.4-cm^{-1} absorptions are therefore assigned to the dibridged Ga_2H_5 isomer (DB in Figure 1). The terminal and bridge-stretching modes of dibridged Ga_2H_5 fall slightly below Ga_2H_6 values as predicted by our calculations. The 1980.5-, 1943.9-, and 782.1-cm^{-1} absorptions produced on photolysis are assigned to the monobridged Ga_2H_5 isomer (MB).

Annealing to 7.5 K with use of a neon overcoat to retain the volatile H_2 solid removed Ga_2H_6 absorptions and left the MB bands, but a final λ > 240 nm irradiation restored Ga_2H_6 and the DB bands (Figure 6f,g).

GaH_2^- and GaH_4^- Anions. The reaction of laser-ablated Ga atoms with H_2 produced a broad band with a sharp peak at 1356.4 cm^{-1} in pure H_2 and a band at 1350.0 cm^{-1} with H_2 in solid neon on deposition: These bands increased slightly on annealing but decreased on photolysis and never restored on further annealing (Figures 1 and 4). In another solid hydrogen experiment with lower laser energy, the 1356.4-cm^{-1} absorption was stronger. Irradiation at λ > 470 nm reduced this band by half and increased the 1773.8-cm^{-1} band, and irradiation at λ > 380 nm continued this trend. In solid hydrogen the 1814.9-cm^{-1} GaH_2 absorption was substantially stronger than the new 1356.4-cm^{-1} band, but in solid neon the 1822.0-cm^{-1} GaH_2 absorption was weaker than the 1350.0-cm^{-1} band. Furthermore, doping with CCl_4 to capture ablated electrons eliminated the 1350.0-cm^{-1} neon matrix absorption and reduced the $GaH_{1,2,3}$ absorptions: New signals were observed for CCl_3^+ at 1046.0 cm^{-1} and CCl_3 at 905.8 cm^{-1} (Figure 5).[36,37] Likewise adding CCl_4 (0.1%) to the hydrogen sample eliminated the 1356.4-cm^{-1} band and produced a sharp 903.5, 900.9 cm^{-1} CCl_3 radical absorption. The CCl_4 molecule preferentially captures ablated electrons and minimizes the yield of molecular anions in these experiments.[22] These 1350-cm^{-1} absorptions are down about 500 cm^{-1} from the neutral terminal Ga−H stretching region and behave like those observed previously for anions. The AlD_2^- anion has been observed in solid D_2, where AlD_2^- reacts to form AlD_4^- on 290-nm photolysis.[17] A new dihydride anion, GaH_2^-, is proposed: Similar dihydride anions, PdH_2^-, SnH_2^-

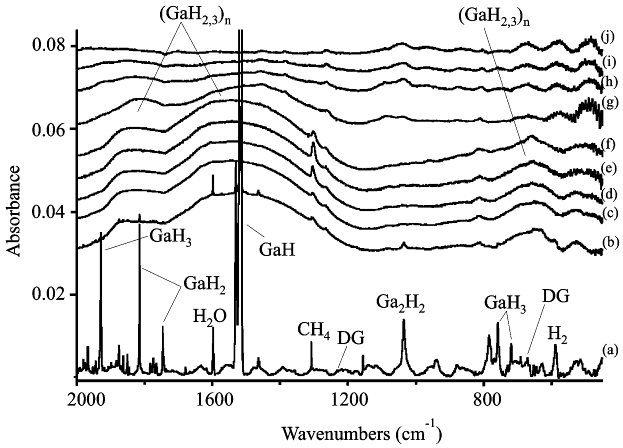

Figure 7. Infrared spectra in the 2000−450 cm^{-1} region for laser-ablated Ga atoms co-deposited with pure normal hydrogen at 3.5 K: (a) spectrum after annealing, $\lambda > 240$ nm irradiation, and annealing to 6.6 K, (b) after annealing to 7.1 K, (c) after annealing to 8.0 K, (d) after annealing to 10.5 K, (e) after warming to 20 K, (f) after warming to 60 K, and (g) after warming to 200, (h) 240, (i) 260, and (j) 290 K.

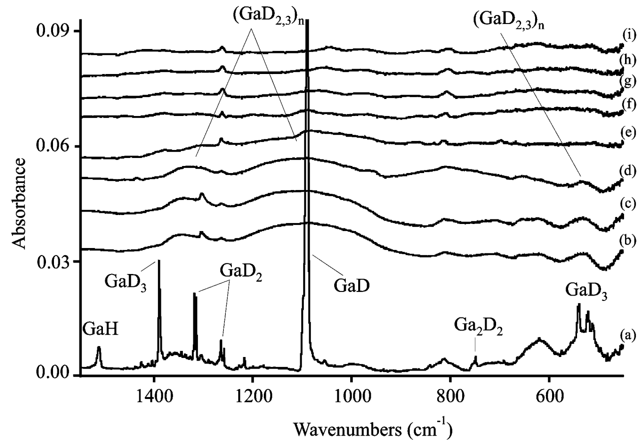

Figure 8. Infrared spectra in the 1550−450 cm^{-1} region for laser-ablated Ga atoms co-deposited with pure normal deuterium at 3.5 K: (a) spectrum after annealing, $\lambda > 240$ nm irradiation, and annealing to 10.4 K, (b) after annealing to 13 K, (c) after warming to 30 K, (d) after warming to 70 K, (e) after warming to 200 K, and (f) after warming to 220, (g) 200, (h) 240, and (i) 295 K.

and PbH_2^-, CuH_2^-, and AgH_2^-, have been trapped in low-temperature matrix samples.[38−40] The D_2 counterparts shift to 973.2 cm^{-1} in pure D_2 and 982.0 cm^{-1} in neon (Figures 3 and 5). The H/D frequency ratios of 1.394 and 1.375 suggest a different interaction in the two matrix hosts. With HD in neon the bands were observed at 1357.9 (Ga−H stretching region) and 982.6 cm^{-1} (Ga−D stretching region) in accord with the presence of a higher frequency symmetric mode for GaH_2^- and GaD_2^-.

Our DFT frequency calculations support this first identification of GaH_2^-. The ground state is found to be $^1A_1$ and the Ga−H bond is predicted slightly longer than for GaH_2 with a H−Ga−H bond angle about 30° smaller than that for the neutral GaH_2. With the B3LYP functional a stronger ν_3 mode at 1388.8 cm^{-1} and a weaker ν_1 mode at 1405.6 cm^{-1} are computed, which match neon matrix and solid hydrogen values very well although the two modes are possibly overlapped in one broad band. A frequency comparison for GaH_2 and GaH_2^- provides further support: B3LYP calculations predict the ν_3 mode of GaH_2^- 457 cm^{-1} lower than that of GaH_2, which is very close to the observed differences of 459 cm^{-1} in solid hydrogen and 472 cm^{-1} in solid neon.

Solid $NaGaH_4$ exhibits strong absorptions at 1760 and 715 cm^{-1},[41] and our DFT calculations predict slightly lower GaH_4^- frequencies. The 1773.8-, 1765.7-, 778.6-, and 774.5-cm^{-1} bands (Figure 1) must be considered for GaH_4^-. These bands are destroyed along with GaH_2^- on 240-nm photolysis and are restored in part with different relative intensities on annealing after photolysis. In another solid hydrogen experiment with lower laser energy the 1356.4-cm^{-1} band was increased (double) relative to the 1773.8-cm^{-1} band. The $H_2 + D_2$ experiment gave similar 1774.9- and 1765.8-cm^{-1} bands plus a weaker 1831.8-cm^{-1} absorption, which decreased together on photolysis. This is the pattern expected for tetrahedral GaH_4^- plus $GaH_2D_2^-$ since the symmetric GaH_2 stretching mode is allowed in $GaH_2D_2^-$ (Table 2). (No peak between 1773.8 and 1765.7 cm^{-1} is found as would be required for the $GaGaH_2$ assignment.[32]) Furthermore the 1787.8- and 1772.8-cm^{-1} neon matrix counterparts are eliminated by doping with CCl_4 (Figure 5), and the hydrogen matrix bands are also eliminated. These bands shift to 1287.8 and 1275.1 cm^{-1} in D_2 and exhibit 1.391 and 1.390 frequency ratios. Hence, the 1773.8- and 774.5-cm^{-1} bands are assigned to GaH_4^- following the observation of AlH_4^- in matrix isolation.[15,17,42] As found for AlD_4^-, $\lambda > 380$ nm irradiation of GaD_2^- in both D_2 and Ne samples increases the GaD_4^- absorptions. Likewise, $\lambda > 380$ nm irradiation reduced GaH_2^- (by half) and increased GaH_4^- (doubled) in solid hydrogen. This lower MH_4^- anion yield is perhaps not surprising as the tetrahydrogallates are known to be less stable than the aluminum analogues. The thermal and chemical stabilities of the BH_4^-, AlH_4^-, and GaH_4^- anions vary with the ability of MH_3 to accept H^-, which follow the trend B > Al ≫ Ga.[10]

It is interesting to compare here the Ga and Al counterpart frequencies for the hydrides observed. For the lower oxidation state species, the AlH_2, AlD_2^-, and AlH frequencies (1822, 1043, and 1599 cm^{-1}, respectively)[15,17] are higher than GaH_2, GaD_2^-, and GaD (1815, 973, and 1517 cm^{-1}, all hydrogen matrix) values. However, for the higher III oxidation state species, the Ga_2H_6, GaH_3, and GaH_4^- frequencies (1995, 1929, and 1774 cm^{-1}) are higher than the Al_2H_6, AlH_3, and AlH_4^- (1931, 1884, and 1638 cm^{-1}) values. Apparently the transition series contraction for Ga is more effective for the higher oxidation state species.

What are the positive counterions for GaH_4^- and GaH_2^- in these systems? The low ionization energy of Ga suggests that Ga^+ is the major cation center. The $Ga^+(H_2)_n$ cation complex was observed at 4108.9 cm^{-1}, and this observation will be discussed in a later paper.

$(GaH_x)_n$ Solids. Warming the matrix above 6.8 K leads to the loss of H_2 and aggregation of the above gallium hydride transient species. Broad absorptions appear at 1800−2000, 1300−1700, and 600−700 cm^{-1} and remain on the window until the hydride material evaporates in the 200−260 K range (Figure 7). With the GaH_3-enriched sample in Figure 2, the major absorption center is 1600 cm^{-1}. The corresponding bands in pure D_2 are slightly sharper: Broad 1300−1400 and 1000−1200 cm^{-1} absorptions form after the deuterium evaporates and remain until the deuteride material evaporates in the 200−260 K range (Figure 8). Downs et al. report broad absorptions at 1422, 1200, and 400 cm^{-1} for an annealed Ga_2D_6 film at 77 K.[12]

The infrared spectrum of annealed solid digallane at 77 K displays broad 1978-cm^{-1} and very broad 1705- and 550-cm^{-1} absorptions. These features are thought to be due to $(GaH_3)_n$ oligomers containing both terminal Ga−H and bridging Ga−H−Ga bonds.[12] Downs and Pulham have suggested a discrete oligomer such as the $(GaH_3)_4$ tetramer as a likely contributor,[1] but the nature of this solid is far from certain. The oligomer prepared here must be slightly different as our precursors are $GaH_{1,2,3}$ as compared to the authentic Ga_2H_6 material. Nevertheless, the present oligomer contains both terminal and bridging bonds based on the observation of one broad band in each region and the major peak shifts higher in the direction of the authentic material peak with increasing proportion of GaH_3. Subsequent work on carefully annealed digallane films produced sharper bands with resolved peaks at 1958, 1929, 1722, 1641, 707, 609, 501, and 441 cm^{-1} in the same region.[43]

Hicks et al.[44] have observed hydrogen adsorption on gallium-rich reconstructed GaAs (001) surfaces as manifested in antisymmetric Ga−H−Ga absorptions in the 1720−1000 cm^{-1} range. These authors point out that the bridging hydrogen stretching frequency varies with the Ga−H−Ga angle.

Theoretical calculations (SCF/DZP) for the Ga_4H_{12} tetramer found a deformed C_{2v} ring (butterfly) structure and extremely intense b_1 and b_2 bridge-bond stretching modes at 1881 and 1893 cm^{-1}.[45] These modes correspond to the parallel $Ga(H)_2Ga$ bridge-bond stretching mode for $H_2Ga(H)_2GaH_2$ calculated at 1400 cm^{-1} and observed at 1273 cm^{-1}.[12,46] Hence, the very strong calculated 1881- and 1893-cm^{-1} absorptions scale to 1700 cm^{-1} and account for the major absorption feature of annealed gallane films. Souter concludes that the vibrational spectrum and physical properties provide strong circumstantial evidence that solid gallane consists of discrete oligomers, possibly tetramers, or of a weakly bound polymer.[43]

Although our absorption bands are similar to those reported for digallane films, differences do exist. When the spectra are superposed, it is clear that our absorption bands overlap the digallane film spectra only slightly, and we must conclude that the oligomer formed when the hydrogen matrix evaporates from our $GaH_{1,2,3}$ sample includes different material from the pure Ga(III) hydride oligomer. Both our Ga−H terminal and Ga−H−Ga vibrations are lower than those found for the digallane films.[12,43] This is consistent with the mixed oxidation state precursors that diffuse and react to make the present hydride film, which include a larger variety of Ga−H−Ga bond angles. Since some of the gallium in our oligomers is hydrogen unsaturated, we label these bands $(GaH_{2,3})_n$.

Other Absorptions. A sharp, weak 1463.5-cm^{-1} band with 1055.8-cm^{-1} D_2 counterpart (H/D frequency ratio 1.386) appears on deposition in pure hydrogen, disappears on photolysis, reappears at the expense of GaH on further annealing, and increases markedly on annealing to 7.5 K with use of a neon overcoat. The same two absorptions are observed with a $H_2 + D_2$ mixture without obvious intermediate. The 1463.5-cm^{-1} band is attributed to a $(GaH)_n$ polymer involving Ga- -Ga linkages and terminal Ga−H bonds.

Photosensitive bands observed at 3972 and 2870 cm^{-1} in solid H_2 and solid D_2 experiments will be assigned to the $(H^-)(H_2)_n$ and $(D^-)(D_2)_n$ anion clusters in a later report.

Reaction Mechanisms. The GaH diatomic molecule is generated from the endothermic ($\Delta E = +38$ kcal/mol)[47] reaction of Ga with H_2, and the reaction is activated by excess energy in the laser-ablated gallium atoms.[48] [The energy differences given are from B3LYP calculations.]

$$Ga\ (^2P) + H_2\ (^1\Sigma_g^+) \rightarrow GaH\ (^1\Sigma^+) + H\ (^2S) \quad [\Delta E = +37\ \text{kcal/mol}] \quad (1)$$

The GaH molecule is trapped in solid hydrogen during deposition and no further reaction with H_2 is observed on annealing although reaction 2 is exothermic by 13 kcal/mol, which indicates that the GaH reaction with H_2 to form GaH_3 requires activation energy. With 240-nm photolysis excited GaH* is generated and the insertion reaction occurs, but reaction 2 is even more efficient with 193-nm excitation. The GaH_3 observed on deposition is due to the reaction of excited GaH formed by the ablation plume.

$$GaH + H_2 \rightarrow GaH_3 \quad [\Delta E = -13\ \text{kcal/mol}] \quad (2)$$

Insertion of ground state Ga into H_2 is exothermic by only 1.5 kcal/mol (reaction 3), but the reaction is not spontaneous in the low-temperature matrix. This insertion reaction is activated with 240-nm photolysis. Note that the GaH_2 molecule is decomposed by 470−700 nm light from the mercury arc.

$$Ga\ (^2P) + H_2\ (^1\Sigma_g^+) \rightarrow GaH_2\ (^2A_1) \quad [\Delta E = -1.5\ \text{kcal/mol}] \quad (3)$$

Electrons are abundant in the plume generated by laser interaction with the metal surface. GaH_2 can capture an electron to give GaH_2^-, which is decreased by 470- and 290-nm radiation, and destroyed by 240-nm photolysis. The calculated 29-kcal/mol electron affinity suggests that this anion is stable and should be observable in the gas phase. Further reaction of GaH_2^- with H_2 can give GaH_4^-, the stable tetrahydrogallate anion, as the reaction of AlH_2^- with H_2 gives AlH_4^-,[15] and we have evidence for GaH_4^- in these experiments. The 380-nm photochemical reaction of GaD_2^- and D_2 (Figure 3) is analogous to the 290-nm activation of AlD_2^- in D_2,[17] and the same photochemical reaction occurs in excess neon (Figure 5). In fact this photochemical reaction is initiated at $\lambda > 470$ nm for both GaH_2^- and GaD_2^-. Alternative preparations for GaH_2^- and GaH_4^- favored in pure hydrogen are the exothermic Lewis acid−base reactions 6 and 7 with hydride anion H^-. The hydride anion is formed in these experiments from electron capture by hydrogen atoms, which is exothermic by 17 kcal/mol.[49] Such reactions contribute to partial restoration of these anions on annealing after photolysis.

$$GaH_2 + e \rightarrow GaH_2^- \quad [\Delta E = -29\ \text{kcal/mol}] \quad (4)$$

$$GaH_2^- + H_2 \rightarrow GaH_4^- \quad [\Delta E = -62\ \text{kcal/mol}] \quad (5a)$$

$$GaD_2^- + D_2 \xrightarrow{470\ \text{nm}} GaD_4^- \quad (5b)$$

$$GaH + H^- \rightarrow GaH_2^- \quad [\Delta E = -19\ \text{kcal/mol}] \quad (6)$$

$$GaH_3 + H^- \rightarrow GaH_4^- \quad [\Delta E = -68\ \text{kcal/mol}] \quad (7)$$

The reaction of Ga_2 with H_2 is spontaneous in solid argon as observed by Himmel et al. These authors suggest that excited triplet $Ga(\mu\text{-}H)_2Ga$ is formed and then quenched to the singlet ground state in the matrix cage.[32] Although laser ablation does not form Ga_2 (ablation temperature too high for Ga_2 to survive), this dimer can be formed on annealing in the matrix. As soon as Ga_2 is formed in the hydrogen matrix, reaction 8 follows.

$$Ga_2\ (X^3\Sigma^+) + H_2 \rightarrow [Ga(\mu\text{-}H)_2Ga\ (T)]^* \rightarrow Ga(\mu\text{-}H)_2Ga\ (^1A_g) \quad [\Delta E = -58\ \text{kcal/mol}] \quad (8)$$

Finally, exothermic dimerizations of GaH_2 and GaH_3 occur (reactions 9 and 10). Clearly the reagent concentrations are critical, and the pure hydrogen matrix provides an ideal medium to form and react GaH_2 and GaH_3, whereas in solid neon and argon GaH_2 and GaH_3 are trapped in the host matrix. Reaction 10 appears to require some activation energy as the UV irradiation that promotes 2 also drives reaction 10: 193-nm radiation is particularly effective in this regard. It may be then that the excited GaH_3 product of reaction 2 continues with reaction 10 when two GaH_3 molecules are in close proximity, but that two cold GaH_3 molecules need activation to form digallane. The reaction of GaH_2 and GaH_3 is also thermochemically favorable and we find evidence for Ga_2H_5 radical production appearing in these experiments before Ga_2H_6 on annealing.

$$GaH_2 + GaH_2 \rightarrow Ga_2H_4 \qquad [\Delta E = -57 \text{ kcal/mol}] \quad (9)$$

$$GaH_3 + GaH_3 \rightarrow H_2Ga(\mu\text{-}H)_2GaH_2 \qquad [\Delta E = -19 \text{ kcal/mol}] \quad (10)$$

$$GaH_2 + GaH_3 \rightarrow H_2Ga(\mu\text{-}H)_2GaH \qquad [\Delta E = -19 \text{ kcal/mol}] \quad (11)$$

Conclusions

Reactions of laser-ablated Ga atoms and normal hydrogen during co-deposition at 3.5 K give GaH as the major product and GaH_2, GaH_3, GaH_2^-, GaH_4^-, and Ga_2H_2 as minor products, as found with the aluminum hydride systsm[15,17] although the photochemical conversion to Al(III) hydrides was more complete.

Irradiation destroyed the GaH_2^- and GaH_4^- anions, decreased GaH and increased GaH_3, and destroyed Ga_2H_2 and produced weak bands for Ga_2H_4 and Ga_2H_6. Ultraviolet photolysis of GaD_2^- and D_2 formed GaD_4^- following a like process in the Al/D_2 system.[17] The GaH_2^- anion is more stable than AlH_2^- (not observed in solid hydrogen), and GaH_4^- is trapped in large yield and appears to be of comparable stability with AlH_4^- in solid hydrogen. These experiments suggest that InH_2^- and possibly InH_4^- can be formed in solid hydrogen. Evidence is presented for two Ga_2H_5 radical structures, namely Ga_2H_6 without one terminal or bridging hydrogen. Although the Ga_2H_6 bands were weak, Ga_2H_6 was identified by matching five infrared absorptions with gas-phase values.[12] This validates the synthetic route to Al_2H_6 using Al atoms and H_2.[15,17]

Warming these samples to remove the H_2 matrix replaces sharp gallium hydride molecular absorptions with broad 1800−2000, 1300−1700, and 600−700 cm^{-1} bands due to higher oligomers containing terminal and bridged Ga−H bonds that are similar to the oligomer formed with authentic digallane.[12]

Acknowledgment. We gratefully acknowledge N.S.F. financial support (Grant CHE 00-78836).

References and Notes

(1) Downs, A. J.; Pulham, C. R. *Chem. Soc. Rev.* **1994**, *1994*, 175.

(2) Chertihin, G. V.; Andrews, L. *J. Phys. Chem.* **1993**, *97*, 10295.

(3) Kurth, F. A.; Eberlein, R. A.; Schnöckel, H.; Downs, A. J.; Pulham, C. R. *J. Chem. Soc., Chem. Commun.* **1993**, 1302.

(4) Xiao, Z. L.; Hauge, R. H.; Margrave, J. L. *Inorg. Chem.* **1993**, *32*, 642.

(5) Pullumbi, P.; Mijoule, C.; Manceron, L.; Bouteiller, Y. *Chem. Phys.* **1994**, *185*, 13.

(6) Pullumbi, P.; Bouteiller, Y.; Manceron, L.; Mijoule, C. *Chem. Phys.* **1994**, *185*, 25.

(7) (a) Urban, R. D.; Magg, U.; Jones, H. *Chem. Phys. Lett.* **1989**, *154*, 135. (b) Urban, R. D.; Birk, H.; Polomsky, P.; Jones, H. *J. Chem. Phys.* **1991**, *94*, 2523.

(8) (a) Zhu, Y. F.; Shehadeh, R.; Grant, E. R. *J. Chem. Phys.* **1992**, *97*, 883. (b) Campbell, J. M.; Dulick, M.; Klapstein, D.; White, J. B.; Bernath, P. F. *J. Chem. Phys.* **1993**, *99*, 8379.

(9) Finhold, A. E.; Bond, A. C.; Schlesinger, H. J. *J. Am. Chem. Soc.* **1947**, *69*, 1199.

(10) Cotton, F. A.; Wilkinson, G.; Murillo, C. A.; Bochmann, M. *Advanced Inorganic Chemistry*, 6th ed.; Wiley: New York, 1999.

(11) Downs, A. J.; Goode, M. J.; Pulham, C. R. *J. Am. Chem. Soc.* **1989**, *111*, 1936.

(12) Pulham, C. R.; Downs, A. J.; Goode, M. J.; Rankin, D. W. H.; Robertson, H. E. *J. Am. Chem. Soc.* **1991**, *113*, 5149.

(13) Breisacher, P.; Siegel, B. *J. Am. Chem. Soc.* **1964**, *86*, 5053.

(14) Turley, J. W.; Rinn, H. W. *Inorg. Chem.* **1969**, *8*, 18.

(15) Andrews, L.; Wang, X. *Science* **2003**, *299*, 2049.

(16) Matzek, W. E.; Musinski, D. F. U.S. Patent 3,883,644, 1975; *Chem. Abstr.* **1975**, *83*, 45418.

(17) Wang, X.; Andrews; L.; Tam, S.; DeRose, M. E.; Fajardo, M. E. *J. Am. Chem. Soc.* **2003**, *125*, 9218.

(18) Shen, M.; Schaefer, H. F., III *J. Chem. Phys.* **1992**, *96*, 2868.

(19) Barone, V.; Orlandini, L.; Adamo, C. *J. Phys. Chem.* **1994**, *98*, 13185.

(20) Souter, P. F.; Andrews, L.; Downs, A. J.; Greene, T. M.; Ma, B.; Schaefer, H. F., III *J. Phys. Chem.* **1994**, *98*, 12824.

(21) Burkholder, T. R.; Yustein, J. T.; Andrews, L. *J. Phys. Chem.* **1992**, *96*, 10089.

(22) Andrews, L.; Citra, A. *Chem. Rev.* **2002**, *102*, 885.

(23) Wang, X.; Andrews, L. *J. Phys. Chem. A* **2003**, *107*, 570.

(24) Frisch, M. J.; Trucks, G. W.; Schlegel, H. B.; Scuseria, G. E.; Robb, M. A.; Cheeseman, J. R.; Zakrzewski, V. G.; Montgomery, J. A., Jr.; Stratmann, R. E.; Burant, J. C.; Dapprich, S.; Millam, J. M.; Daniels, A. D.; Kudin, K. N.; Strain, M. C.; Farkas, O.; Tomasi, J.; Barone, V.; Cossi, M.; Cammi, R.; Mennucci, B.; Pomelli, C.; Adamo, C.; Clifford, S.; Ochterski, J.; Petersson, G. A.; Ayala, P. Y.; Cui, Q.; Morokuma, K.; Malick, D. K.; Rabuck, A. D.; Raghavachari, K.; Foresman, J. B.; Cioslowski, J.; Ortiz, J. V.; Stefanov, B. B.; Liu, G.; Liashenko, A.; Piskorz, P.; Komaromi, I.; Gomperts, R.; Martin, R. L.; Fox, D. J.; Keith, T.; Al-Laham, M. A.; Peng, C. Y.; Nanayakkara, A.; Gonzalez, C.; Challacombe, M.; Gill, P. M. W.; Johnson, B. G.; Chen, W.; Wong, M. W.; Andres, J. L.; Head-Gordon, M.; Replogle, E. S.; Pople, J. A. *Gaussian 98*, revision A.6; Gaussian, Inc.: Pittsburgh, PA, 1998.

(25) (a) Krishnan, R.; Binkley, J. S.; Seeger, R.; Pople, J. A. *J. Chem. Phys.* **1980**, *72*, 650. (b) Frisch, M. J.; Pople, J. A.; Binkley, J. S. *J. Chem. Phys.* **1984**, *80*, 3265.

(26) Becke, A. D. *Phys. Rev. A* **1988**, *38*, 3098.

(27) Perdew, J. P.; Wang, Y. *Phys. Rev. B* **1992**, *45*, 13244.

(28) Becke, A. D. *J. Chem. Phys*. **1993**, *98*, 5648.

(29) Lee, C.; Yang, E.; Parr, R. G. *Phys. Rev. B* **1988**, *37*, 785.

(30) Stevens, P. J.; Devlin, F. J.; Chablowski, C. F.; Frisch, M. J. *J. Phys. Chem*. **1994**, *98*, 11623.

(31) Hauge, R. H.; Kauffman, J.W.; Margrave, J. L. *J. Am. Chem. Soc.* **1980**, *102*, 6005.

(32) Himmel, H.-J.; Manceron, L.; Downs, A. J.; Pullumbi, P. *J. Am. Chem. Soc.* **2002**, *124*, 4448.

(33) Lammertsma, K.; Leszczynski, J. *Inorg. Chem.* **1990**, *29*, 5543.

(34) Xie, Y.; Grev, R. S.; Gu, J.; Schaefer, H. F., III; Schleyer, P. v. R.; Su, J.; Li, X.-W.; Robinson, G. H. *J. Am. Chem. Soc.* **1998**, *120*, 3773.

(35) Duncan, J. L. *J. Mol. Spectrosc*. **1985**, *113*, 63.

(36) Andrews, L. *J. Phys. Chem.* **1967**, *71*, 2761.

(37) Lugez, C. L.; Jacox, M. E.; Johnson, R. D. *J. Chem. Phys.* **1998**, *109*, 7147 and references therein.

(38) Andrews, L.; Wang, X.; Alikhani, M. E.; Manceron, L. *J. Phys. Chem. A* **2001**, *105*, 3052.

(39) Wang, X.; Andrews, L.; Chertihin, G. V.; Souter, P. F. *J. Phys. Chem. A* **2002**, *106*, 6302.

(40) Andrews, L.; Wang, X. *J. Am. Chem. Soc.* **2003**, *125*, 11751.

(41) Shirk, A. E.; Shirver, D. F. *J. Am. Chem. Soc.* **1973**, *95*, 5904.

(42) Pullumbi, P.; Bouteiller, Y.; Manceron, L. *J. Chem. Phys.* **1994**, *101*, 3610.

(43) Souter, P. F., D. Phil. Thesis, University of Oxford, 1995.

(44) Hicks, R. F.; Qi, H.; Fu, Q.; Han, B.-K.; Li, L. *J. Chem. Phys.* **1999**, *110*, 10498.

(45) Liang, C.; Davy, R. D.; Schaeffer, H. F., III *Chem. Phys. Lett.* **1989**, *159*, 393.

(46) Shen, M.; Schaeffer, H. F., III *J. Chem. Phys.* **1992**, *96*, 2868.

(47) Huber, K. P.; Herzberg, G. *Constants of Diatomic Molecules*; Van Nostrand: Princeton, NJ, 1979.

(48) Kang, H.; Beauchamp, J. L. *J. Phys. Chem.* **1985**, *89*, 3364.

(49) Berry, R. S. *Chem. Rev.* **1969**, *69*, 533.